Formation of Linear Water Chains on Ni(110)

Nikki Gerrard, Kallum Mistry, George R. Darling and Andrew Hodgson*

Surface Science Research Centre and Department of Chemistry, University of Liverpool, Liverpool L69 3BX, UK

* ahodgson@liverpool.ac.uk

Abstract

Materials that bind strongly to water structure the contact layer, modifying its chemical and physical properties in a manner that depends on the symmetry and reactivity of the surface. Although detailed models have been developed for several inert surfaces, much less is known about reactive surfaces, particularly those with a different symmetry to ice. Here we investigate water adsorption on a rectangular surface, Ni(110), an active reforming catalyst that interacts strongly with water. Instead of forming a network of H-bonded cyclic rings, water forms flat 1D water chains, leaving half the Ni atoms exposed. Second layer water also follows the surface symmetry, forming chains of alternating pentamer and heptamer rings in preference to an extended 2D structure. This behaviour is different to that found on other surfaces studied previously and is driven by the short lattice spacing of the solid and the strength of the Ni-water bond.

TOC Graphic

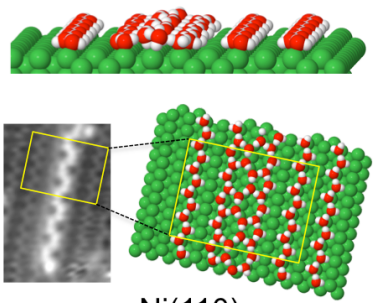

Keywords: Nickel, Water, Interface, Scanning tunneling microscopy

Text

Water confined in low dimensional structures at a solid interface, for example within a pore or nano-tube, can display dynamic properties quite different to bulk water [1-3], with potentially useful characteristics [4-5]. This change in behaviour is driven by the way in which the solid surface modifies and constrains water's hydrogen bonding structure, making the ability to predict this response an important ambition in designing technological interfaces. However, water structure prediction remains a challenge [6], limited by the flexibility of water-water hydrogen bonds and the sensitivity of its structure to the particular environment [7]. Investigating the wetting of well-defined model surfaces allows the effect of lattice parameter, symmetry and binding energy to be explored separately to discover to what extent these factors affect the water structure [8-15]. Manipulating the surface offers the ability to deliberately control the structure and properties of interface water, for example to encourage 3D ice growth [16], change the friction [3] or transport properties [4, 17-18] as desired.

Whereas water is inert on the close packed faces of the noble metals, where wetting has been studied in detail [7], the open surfaces are more reactive. Ni(110) is an active catalyst for re-forming reactions, creating interest in how water adsorbs and dissociates on this surface [19-20]. Although water was originally thought to form a distorted 2D hexagonal H-bond network [21], subsequent work showed this is a partially dissociated OH/H_2O phase [22], leaving the nature of intact water structures unclear [21-27]. The related Cu(110) surface, where dissociation is slow, is rather better understood. In place of the more typical hexagonal structures, water forms chains of face sharing pentamer rings that match the short atomic spacing of Cu [28], leading to the prediction that the reduced metal spacing and strong water-Ni bond of Ni(110) [19] will make water pentamer chains yet more stable [28]. Here we report STM measurements of intact water adsorption on Ni(110), using DFT to explore the structures observed and low current LEED to relate these results to earlier studies. We show that, instead of forming a network based on cyclic rings, water creates linear two-coordinate chains along the close packed Ni rows, saturating the surface with half the Ni atoms still exposed. This unusual structure has a dramatic effect on further water adsorption, with second layer growth forming 1D chains containing pentamer and heptamer rings, rather than an extended 2D structure. The combination of a rectangular surface template and strong water-Ni bond creates an environment that strongly favours linear 1D structures over the 2D water structures more commonly observed on other metal surfaces [8].

Depositing water onto the Ni(110) surface at 80 K results in the growth of extended domains of water, shown in Figure 1a,b. Despite the low adsorption temperature, the water structure is ordered, forming bright chains along the $[1\bar{1}0]$ direction. The water chains sit above the Ni closed packed rows, with the majority of the chains having a zigzag repeat with a period of twice the Ni spacing. Only a few bright, mobile features appear ca. 0.7 Å above the first layer and are attributed to water that is trapped in the second layer, implying that water preferentially wets this surface rather than forming multilayer islands. Perpendicular to the close packed Ni rows, the bright chains have a regular spacing of 2 times the Ni row spacing, with no structure appearing between the chains.

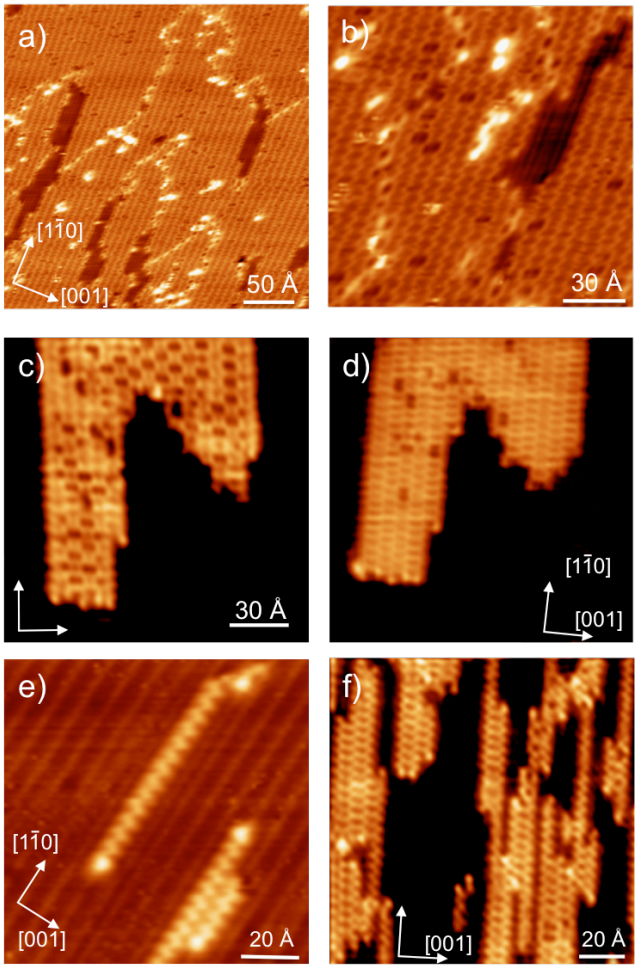

Fig. 1 STM images showing water adsorbed on Ni(110) at 80 K. a,b) just under 0.5 monolayer of water showing small regions of bare Ni (the darker patches) and a few bright, relatively mobile features associated with water adsorbed above the first layer. c,d) a low coverage (0.07 monolayer) of water adsorption at 80 K. Image (c) is recorded immediately after dosing water and shows formation of 2D islands that contain darker voids, while d) shows the same island 70

minutes later (these images are uncorrected for thermal drift). e,f) Isolated 1D chains formed in the presence of a small amount of O that pins the water chains and reduces island formation. Doubling of the Ni period to 7Å along [001] in some regions of (e) is caused by H induced Ni row pairing, see the Methods for more details. The apparent height of the water chains above Ni is between 50 and 60 pm and the scan conditions were a,b) 215 pA, -0.380 V, c) 123 pA, -0.034 V, d) 256 pA, -0.030 V, e) 110 pA, -0.22 V, and f) 175 pA, -0.090 V.

Despite the remarkably high degree of order, the water layer contains defects that provide an insight into the nature of the structure. In particular, darker voids appear occasionally between the chains, as shown in Fig. 1b, often forming a regular pattern. An example of such an ordered arrangement can be seen in the small water island shown in Figure 1c, recorded immediately after water deposition at 80 K. The structure in the top centre of the island consists of bright chains with a repeat of 4 times the Ni lattice parameter along the Ni close packed rows, forming a (4x4) structure, while the row of dark voids on the top right of the island has a 3 times repeat. Figure 1d shows the same island an hour later; the majority of the dark voids near to an island edge have disappeared, with no apparent change in the island area, leaving bright zigzag chains along the Ni rows. Depositing water at a higher temperature reduces the number of defect features, though they persist inside large islands even at 150 K. The dark voids are associated with a different local repeat along $[1\bar{1}0]$ and form freely during water adsorption, but are metastable, slowly annealing out of the water structure at 80 K. LEED patterns for this surface (see SI, Fig. S1) show diffuse (2x2) beams that are streaked along the [001] direction, reflecting disorder in the registry between zigzag chains on different Ni rows. When the Ni(110) surface has a small amount of O present, as shown in Fig. 1e,f, water forms isolated chains or small 2D structures, pinned by bright features (presumably OH), rather than extended 2D domains of pure water. Irrespective of the details of adsorption, the STM images all show water forming chains along the Ni close packed direction, separated from the next chain by 7Å (2 lattice repeats along [001]) - too great a distance to be explained by hydrogen bond formation.

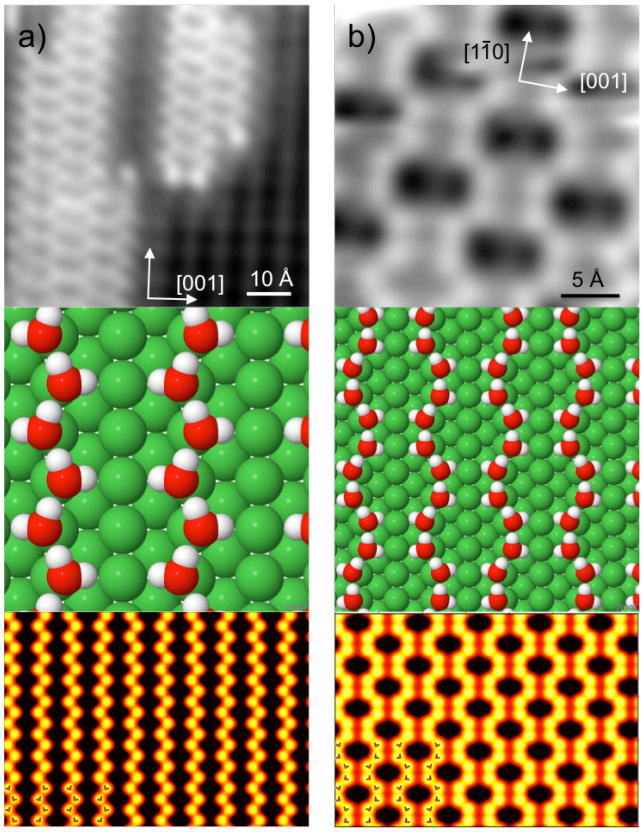

Fig. 2. The panels (top to bottom) show an STM image, the most stable calculated structure for water and its filled state STM simulation for 0.5 monolayer water in a) a (2x4) and b) a (4x4) unit cell, with binding energies of 0.871 and 0.864 eV/water respectively. STM images were recorded after adsorption at 80 K with a) 175 pA, -0.09 V and b) 240 pA, -0.38 V.

In order to understand this behaviour we investigated the stability of possible water structures using DFT. Fully hydrogen bonded networks containing 1 monolayer of water, as well as lower coverage structures were considered, and these are summarised in the SI, see Figs. S3 to S6. The most stable structures we found with a 2 or 4 times repeat along the Ni rows are shown in Fig. 2 and consist of 0.5 monolayer water adsorbed flat near the Ni top site, forming hydrogen bonded chains along the Ni rows. Each water chain is separated from its neighbour by a row of bare Ni. The two different structures differ only in the lateral arrangement of the uncoordinated H atoms. Whereas the ‘zigzag’ chain (Fig. 2a) has the O atom and free H alternating to each side of the chain with a 2 unit repeat, the ‘wiggly’ chain (Fig. 2b) as a 4 unit repeat, with pairs of water molecules alternating along each side of the Ni row. Despite having just two H-bonds per water molecule, these flat water chains are 0.034 eV/water more stable than the best fully hydrogen bonded 2D network with 3 hydrogen bonds per water (see SI Fig S4). Moreover, formation of flat 1D water chains along the Ni rows immediately explains all the different ordered structures observed experimentally. Since the binding energy is similar for both chain repeats

(Fig. S3), combining the two units with different phase on neighbouring chains can create all the different structures observed, something that is not possible with a 2D network. Although the water coverage is low, with half of the top layer Ni still exposed, it is not possible to adsorb additional water to create a complete 2D network without reducing the overall binding energy of the chain structure (see SI, Fig. S4 for more details). While the DFT calculations reproduce closely the structure of the water chains, they are not able to describe accurately the weak interactions assembling the chains into 2D islands. In fact the calculations predict the binding energy increases very slightly, by 0.004 meV/water as the chains are separated one unit along [001] (see SI, Fig. S3), but this energy change is less than the accuracy of the calculations.

The assignment of this first layer water structure to flat, low coordinate water chains also allows us to understand the unusual structures formed during second layer growth. Figure 3a shows an image of the surface for a coverage just above 0.5 monolayer water. Bright features appear *ca.* 0.7 Å above the first layer water structure, forming linear chains that can extend up to 100 nm along the Ni close packed direction (see SI, Fig. S2). Figure 3b shows detail of one of these chains. The second layer water lies along the gap between two first layer water chains, appearing only in (2x4) regions of the first layer where water has a simple zigzag chain arrangement and avoiding the (4x4) void structure (e.g. see central region, Fig 3a). The second layer chains never come closer than 4 Ni rows apart, and have a very characteristic appearance, with large rings appearing on alternating sides of the chain and a 4 unit repeat along the chain. LEED patterns for the second layer (Fig. S1b) show the same streaked (2x2) beams as for the first layer but with additional weak spots at the (0.75, 0) positions, consistent with a 4 unit repeat along $[1\bar{1}0]$. STM images taken as the coverage is increased towards 1 monolayer water show the chains coexisting alongside disordered 2D domains that have a similar contrast. Partial ordering occurs as the surface is annealed to 140 – 150 K, (Fig. 4), but dissociation starts to occur at higher temperature [22] and neither the 2D structure nor the LEED pattern fully order.

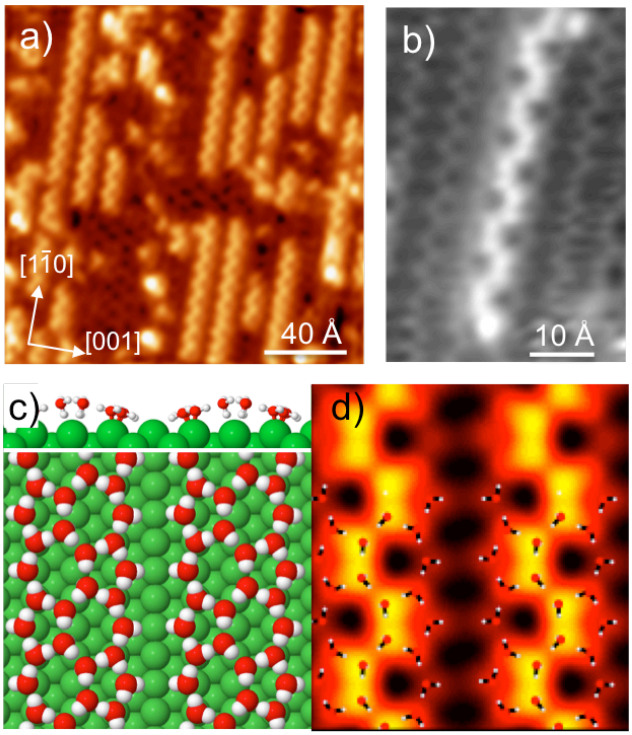

Fig. 3. a,b) STM images showing second layer water growth at 80 K forming 1D chains that image *ca.* 0.7 Å above the first layer water. (c) the structure calculated by DFT with a binding energy of 0.874 eV/water and (d) the corresponding STM simulation for the second layer water chains. The STM images were recorded at V=-0.2 V and I=240 pA.

Figure 3c shows the most stable 1D chain structure found for second layer water in DFT calculations. The structure consists of a H-down water chain, with a 4 unit repeat, inserted into the gap between two flat, zigzag first layer water chains to form a row of alternating pentamer-heptamer rings. This structure has a binding energy (0.874 eV/water) that is indistinguishable from that of the original flat chain structure and more stable than other possible 1D chains or extended 2D water networks considered (see SI, Figs. S4 and S5). The H-down water sits 0.68 Å above the original flat water chains, similar to the contrast seen in STM (Fig. 3) and a simulation of the second layer chain reproduces the characteristic shape seen in experimental images (compare Fig. 3 b and d). The structure of the added row water also helps explain why second layer chains do not form alongside each other. In order to allow water along the outside of the structure to maintain a strong bond to Ni and yet still donate H to water in the H-down chain, the first layer water tilts, with the uncoordinated H atoms on the outside of the chain pointing down towards the bare Ni row while the inside H tilts up to form a H-bond (Fig. 3c). Adding a further water chain along the vacant Ni channel would prevent this relaxation, hindering H-bond formation, and the resulting 2D structure (Fig. S4d) is 0.048 eV/water less

stable than the pentamer-heptamer chains. Of the other possible structures calculated for 1 monolayer of water, the most stable networks have water arranged either as pairs or chains of flat and H-down water, creating distorted hexagonal networks with different corrugations (see Fig. S4 a-d). 2D structures of this type have similar binding energies (between 0.837 and 0.831 eV/water), suggesting that these structures may contribute to the disordered 2D islands observed at higher coverage (Fig. 4). In contrast, forming an ordered c(2x2) bilayer of the type originally proposed on Ni(110) [21] (Fig. S4 e,f) forces water in the first layer to tilt out of plane to complete the hydrogen bond network and these structures are unfavourable by a further 0.040 eV/water.

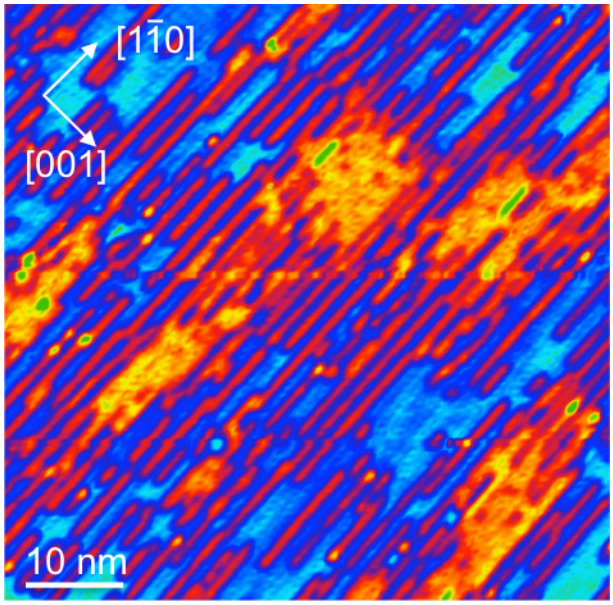

Fig. 4. STM image of *ca.* 0.75 monolayer water after annealing to 140 K. The second layer chains and domains are shown in red-yellow, while the flat first layer chains appear in light/dark blue. STM image recorded at 80 K with I=60 pA and V=0.48 V.

Although simple two-coordinate water chains have been seen as metastable structures on other metal surfaces below 20 K [29-30], this is the first direct observation of water forming stable 1D chains in preference to cyclic structures on a metal surface. Moreover, the structures formed on Ni(110) are quite different to the 1D pentamer chains found on Cu(110) [28, 31], despite these surfaces having a similar lattice spacing and reactivity. Forming a pentamer chain along [001] increases the average H-bond coordination from 2 to 2.67, but only two thirds of the water now bonds directly to the metal, with the other third rotated out of plane to complete the H-bond network (see SI, Fig. S6). Whereas this is favourable on Cu(110), the stronger water-metal interaction (0.63 eV/water[19] on Ni compared to 0.49 eV/water on Cu) shifts the balance in favour

of forming flat, 2-coordinate water chains along the close packed Ni rows. DFT calculations of the two structures on Ni(110) slightly favour pentamer chain formation (by 0.010 eV/water, see SI Fig. S6). This preference to form pentamer chains persists when using different functionals (see SI Table 1), emphasising once again that while such calculations provide valuable insight into the bonding behaviour, they are not sufficiently accurate to predict water structures *a priori* without suitable experimental constraint.

The observation of flat water chains on Ni(110) also helps clarify earlier experimental observations, providing an insight into the behaviour of water on this surface. Callen *et al.* found the water structure is IR inactive below 0.5 monolayer, but became active as the coverage increased to 1 monolayer [25]. This behaviour is consistent with the water chains being flat on the surface and therefore IR inactive, while the next 0.5 monolayer adsorbs in an IR active, H-down configuration in the second layer. In addition, nuclear reaction analysis measurements found that the first layer saturated at 0.5 monolayer coverage [24], the same as the chain structures reported here. This agreement is surprising, since some dissociation would be expected under the conditions used previously [22, 32], and suggests further investigation of the mixed OH/H_2O phases is necessary. Flat water chains analogous to those seen on Ni(110) also appear as the backbone of the OH/H_2O chains formed on Cu(110) [33], reflecting the stability of this water arrangement. Linear chains have previously been proposed at low coordinate metal step sites [34], but cyclic structures are also stabilised [35-36] and complex 2D networks have been found extending across multiple step sites [37]. The stability of the two layer water chains shown in Fig. 3, also suggests a new way in which water might wet corrugated surfaces. By forming a structure that bridges between two Ni rows, this network increases its average H-bond coordination while still having 2/3 of the water bound at the optimum surface site. We expect that linear structures of this type will also be favoured on suitable stepped surfaces, for example where the step spacing allows water to form a 2D H-bond network pinned between two steps.

In conclusion, this study shows that water adsorbs on a Ni(110) surface to produce a tightly bound, low coordinate 1D H-bond structure that optimises the water-surface interaction but leaves half the Ni sites exposed. The tightly bound first layer constrains second layer growth, creating narrow 2D chains that retain the same first layer structure. These results offer an insight into the way in which water adapts its structure to bind on reactive surfaces, about which little is known. We believe that the structures formed here will have direct analogues on other tightly binding surfaces, including low symmetry surfaces where the binding energy varies

periodically across the surface, such as stepped surfaces and biological ice forming or inhibiting proteins.

Methods

The Ni(110) surface (Surface Preparation Laboratory) was cleaned by Ar^+ ion sputtering and annealing to 950 K. STM measurements were carried out in a Createc STM with the sample held at 80 K during adsorption and imaging, prior to annealing to different temperatures [37]. STM images were recorded in constant current mode at 80 K with an electrochemically etched tungsten tip. At 80 K background hydrogen in the STM cryostat slowly deposits on the surface over several days, changing exposed Ni from its original (1x1) termination to the (1x2) row paired arrangement. All the structures reported here were formed on the (1x1) surface and did not change in appearance as H adsorbed on the remaining exposed Ni surface. STM images of water were insensitive to the scan conditions between ±0.5 V and I<250 pA, where the structures were not perturbed by the tip. LEED and thermal desorption measurements were carried out in a second chamber, equipped with a calibrated molecular beam to dose known amounts of water onto the surface. The water beam was calibrated against the 1 monolayer water structure formed on Cu(511) [37], and allowed the coverage to be chosen to ±2% monolayer. LEED patterns were measured at currents of less than 1 nA, to avoid electron induced dissociation, using a low current, dual micro-channel plate LEED system (OCI).

Calculations were performed using VASP [38-39] with the PAW method [40-41] using the optB86b-vdW exchange-correlation functional [42-43], with an 11x15 Monkhorst-Pack *k*-point set for a (2x2) unit cell (5x15 *k*-points for (4x2) and 5x7 *k*-points for (4x4) unit cells) and a 400 eV cutoff. The slabs were 6 Ni layers thick (3 layers fixed, 3 relaxed) with a vacuum gap >20 Å above the upper water layer. Dipole corrections were applied perpendicular to the slab. The optB86b-vdW functional includes van der Waals interactions, which are known to be important in stabilizing surface adsorption relative to 3D ice formation [43-44], and has a similar performance to other vdW functionals for systems where physisorption is important [45]. Trial structures were converged so that the forces on the atoms were < 0.01 eV/Å. The water binding energy (E_b), quoted in the text is defined by

$$-E_b = (E_{slab}^{tot} - E_{Ni} - n_{H_2O}E_{H_2O})/n_{H_2O} \qquad (1)$$

where E_{slab}^{tot} is the energy of the final slab, E_{Ni} is the energy of the metal slab alone and E_{H_2O} the energy of an isolated water in vacuum. To allow for a rapid scan through possible configurations of the water overlayer, the calculations were not spin polarized. We tested the effects of spin polarization by computing binding energies for the structures in Figs. 2, 3, S3b, S4b and S6

using the PBE functional including Grimme D3 dispersion corrections [46] (details are given in the SI). Although the absolute binding energies change slightly, as expected, the relative stability of the different structures remain the same. STM simulations were performed using the Tersoff Hamann approximation [47-48], which approximates the tunnel current as the integral of the local density of states from the bias voltage to the Fermi energy.

Acknowledgements

This work was supported by the EPSRC via grant EP/K039687/1 and SCG10020 and used the UK Materials and Molecular Modelling Hub for computational resources, via our membership of the UK's HEC Materials Chemistry Consortium funded by EPSRC (EP/L000202, EP/R029431**)**, which is partially funded by EPSRC (EP/P020194). Work was also undertaken on Barkla, part of the High Performance Computing facilities at the University of Liverpool, UK.

Supporting Information Available: Details of the LEED patterns, STM images and supporting DFT calculations are provided.

References

1. Kolesnikov, A. I.; Anovitz, L. M.; Hawthorne, F. C.; Podlesnyak, A.; Schenter, G. K., Effect of fine-tuning pore structures on the dynamics of confined water. *J. Chem. Phys.* **2019,** *150* (20), 204706.

2. Prisk, T. R.; Hoffmann, C.; Kolesnikov, A. I.; Mamontov, E.; Podlesnyak, A. A.; Wang, X.; Kent, P. R. C.; Anovitz, L. M., Fast Rotational Diffusion of Water Molecules in a 2D Hydrogen Bond Network at Cryogenic Temperatures. *Phys. Rev. Lett.* **2018,** *120* (19), 196001.

3. Lee, H.; Ko, J. H.; Choi, J. S.; Hwang, J. H.; Kim, Y. H.; Salmeron, M.; Park, J. Y., Enhancement of Friction by Water Intercalated between Graphene and Mica. *Journal of Physical Chemistry Letters* **2017,** *8* (15), 3482.

4. Yang, Q.; Su, Y.; Chi, C.; Cherian, C. T.; Huang, K.; Kravets, V. G.; Wang, F. C.; Zhang, J. C.; Pratt, A.; Grigorenko, A. N.; Guinea, F.; Geim, A. K.; Nair, R. R., Ultrathin graphene-based membrane with precise molecular sieving and ultrafast solvent permeation. *Nature Mat.* **2017,** *16* (12), 1198.

5. Abraham, J.; Vasu, K. S.; Williams, C. D.; Gopinadhan, K.; Su, Y.; Cherian, C. T.; Dix, J.; Prestat, E.; Haigh, S. J.; Grigorieva, I. V.; Carbone, P.; Geim, A. K.; Nair, R. R., Tunable sieving of ions using graphene oxide membranes. *Nature Nanotechnology* **2017,** *12* (6), 546.

6. Brandenburg, J. G.; Zen, A.; Fitzner, M.; Ramberger, B.; Kresse, G.; Tsatsoulis, T.; Gruneis, A.; Michaelides, A.; Alfe, D., Physisorption of Water on Graphene: Subchemical Accuracy from Many-Body Electronic Structure Methods. *Journal of Physical Chemistry Letters* **2019,** *10* (3), 358.

7. Shimizu, T. K.; Maier, S.; Verdaguer, A.; Velasco-Velez, J. J.; Salmeron, M., Water at surfaces and interfaces: From molecules to ice and bulk liquid. *Progress in Surface Science* **2018,** *93* (4), 87.

8. Ma, R. Z.; Cao, D. Y.; Zhu, C. Q.; Tian, Y.; Peng, J. B.; Guo, J.; Chen, J.; Li, X. Z.; Francisco, J. S.; Zeng, X. C.; Xu, L. M.; Wang, E. G.; Jiang, Y., Atomic imaging of the edge structure and growth of a two-dimensional hexagonal ice. *Nature* **2020,** *577* (7788), 60.

9. Heidorn, S. C.; Lucht, K.; Bertram, C.; Morgenstern, K., Preparation-Dependent Orientation of Crystalline Ice Islands on Ag(111). *J. Phys. Chem. B* **2018,** *122* (2), 479.

10. Maier, S.; Lechner, B. A. J.; Somorjai, G. A.; Salmeron, M., Growth and Structure of the First Layers of Ice on Ru(0001) and Pt(111). *J. Am. Chem. Soc.* **2016,** *138* (9), 3145.

11. Yu, X. J.; Schwarz, P.; Nefedov, A.; Meyer, B.; Wang, Y. M.; Woll, C., Structural Evolution of Water on ZnO(10-10): From Isolated Monomers via Anisotropic H-Bonded 2D and 3D Structures to Isotropic Multilayers. *Ang. Chem.* **2019,** *58*, 17751.

12. Kaya, S.; Schlesinger, D.; Yamamoto, S.; Newberg, J. T.; Bluhm, H.; Ogasawara, H.; Kendelewicz, T.; Brown, G. E.; Pettersson, L. G. M.; Nilsson, A., Highly Compressed Two-Dimensional Form of Water at Ambient Conditions. *Scientific Reports* **2013,** *3*, 1074.

13. McBride, F.; Darling, G. R.; Pussi, K.; Hodgson, A., Tailoring the structure of water at a metal surface: a structural analysis of the water bilayer formed on an alloy template. *Phys. Rev. Lett.* **2011,** *106* (22), 226101.

14. Massey, A.; McBride, F.; Darling, G. R.; Nakamura, M.; Hodgson, A., The role of lattice parameter in water adsorption and wetting of a solid surface. *Phys. Chem. Chem. Phys.* **2014,** *16* (43), 24018.

15. Gerrard, N.; Gattinoni, C.; McBride, F.; Michaelides, A.; Hodgson, A., Strain Relief during Ice Growth on a Hexagonal Template. *J. Am. Chem. Soc.* **2019**, 8599.

16. Lin, C.; Corem, G.; Godsi, O.; Alexandrowicz, G.; Darling, G. R.; Hodgson, A., Ice nucleation on a corrugated surface. *J. Am. Chem. Soc.* **2018,** *140* (46), 15804.

17. Radha, B.; Esfandiar, A.; Wang, F. C.; Rooney, A. P.; Gopinadhan, K.; Keerthi, A.; Mishchenko, A.; Janardanan, A.; Blake, P.; Fumagalli, L.; Lozada-Hidalgo, M.; Garaj, S.; Haigh, S. J.; Grigorieva, I. V.; Wu, H. A.; Geim, A. K., Molecular transport through capillaries made with atomic-scale precision. *Nature* **2016,** *538* (7624), 222.

18. Bertram, C.; Fang, W.; Pedevilla, P.; Michaelides, A.; Morgenstern, K., Anomalously Low Barrier for Water Dimer Diffusion on Cu(111). *Nano Letters* **2019,** *19* (5), 3049.

19. Zhu, L.; Liu, C. L.; Wen, X. D.; Li, Y. W.; Jiao, H. J., Coverage dependent structure and energy of water dissociative adsorption on clean and O-pre-covered Ni (100) and Ni(110). *Catalysis Science & Technology* **2019,** *9* (17), 4725.

20. Mohsenzadeh, A.; Richards, T.; Bolton, K., DFT study of the water gas shift reaction on Ni(111), Ni(100) and Ni(110) surfaces. *Surf. Sci.* **2016,** *644*, 53.

21. Benndorf, C.; Madey, T. E., Adsorption Of H2O On Clean And Oxygen-Predosed Ni(110). *Surf. Sci.* **1988,** *194* (1-2), 63.

22. Pirug, G.; Knauff, O.; Bonzel, H. P., Structural and Chemical Aspects of H2O Adsorption on Ni(110). *Surf. Sci.* **1994,** *321* (1-2), 58.

23. Olle, L.; Salmeron, M.; Baro, A. M., The Adsorption And Decomposition Of Water On Ni(110) Studied By Electron-Energy Loss Spectroscopy. *J. Vac. Sci. Techn. A* **1985,** *3* (4), 1866.

24. Callen, B. W.; Griffiths, K.; Memmert, U.; Harrington, D. A.; Bushby, S. J.; Norton, P. R., The Adsorption Of Water On Ni(110) - Monolayer, Bilayer And Related Phenomena. *Surf. Sci.* **1990,** *230* (1-3), 159.

25. Callen, B. W.; Griffiths, K.; Norton, P. R., Reorientation Of Chemisorbed Water On Ni(110) By Hydrogen-Bonding To 2nd-Layer. *Phys. Rev. Lett.* **1991,** *66* (12), 1634.

26. Callen, B. W.; Griffiths, K.; Kasza, R. V.; Jensen, M. B.; Thiel, P. A.; Norton, P. R., Structural Phenomena Related to Associative and Dissociative Adsorption of Water on Ni(110). *J. Chem. Phys.* **1992,** *97* (5), 3760.

27. Pangher, N.; Schmalz, A.; Haase, J., Structure Determination Of Water Chemisorbed On Ni(110) By Use Of X-Ray-Absorption Fine-Structure Measurements. *Chem. Phys. Lett.* **1994,** *221* (3-4), 189.

28. Carrasco, J.; Michaelides, A.; Forster, M.; Raval, R.; Hodgson, A., A Novel One Dimensional Ice Structure Built from Pentagons. *Nature Mat.* **2009,** *8*, 427.

29. Dong, A. N.; Sun, L. H.; Tang, X. Q.; Yao, Y. K.; An, Y.; Hao, D.; Shan, X. Y.; Lu, X. H., Observation of Simplest Water Chains on Surface Stabilized by a Hydroxyl Group at One End. *Chinese Physics Letters* **2019,** *36* (11), 116801.

30. Kumagai, T.; Okuyama, H.; Hatta, S.; Aruga, T.; Hamada, I., Water clusters on Cu(110): Chain versus cyclic structures. *J. Chem. Phys.* **2011,** *134* (2), 024703.

31. Yamada, T.; Tamamori, S.; Okuyama, H.; Aruga, T., Anisotropic water chain growth on Cu(110) observed with scanning tunneling microscopy. *Phys. Rev. Lett.* **2006,** *96* (3), 036105.

32. Gerrard, N., An Investigation into the Hydration and Growth of Ice Layers on Metal Surfaces using Low Temperature Scanning Tunnelling Microscopy. *Ph.D. thesis, University of Liverpool* **2019**.

33. Forster, M.; Raval, R.; Carrasco, J.; Michaelides, A.; Hodgson, A., Water-hydroxyl phases on an open metal surface: breaking the ice rules. *Chem. Sci.* **2012,** *3*, 93.

34. Endo, O.; Nakamura, M.; Sumii, R.; Amemiya, K., 1D Hydrogen Bond Chain on Pt(211) Stepped Surface Observed by O K-NEXAFS Spectroscopy. *J. Phys. Chem. C* **2012,** *116* (26), 13980.

35. Kolb, M. J.; Wermink, J.; Calle-Vallejo, F.; Juurlink, L. B. F.; Koper, M. T. M., Initial stages of water solvation of stepped platinum surfaces. *Phys. Chem. Chem. Phys.* **2016,** *18* (5), 3416.

36. Shiotari, A.; Sugimoto, Y.; Kamio, H., Characterization of two- and one-dimensional water networks on Ni(111) via atomic force microscopy. *Phys. Rev. Materials* **2019,** *3* (9) 093001.

37. Lin, C.; Avidor, N.; Corem, G.; Godsi, O.; Alexandrowicz, G.; Darling, G. R.; Hodgson, A., Two-Dimensional Wetting of a Stepped Copper Surface. *Phys. Rev. Lett.* **2018,** *120*, 076101.

38. Kresse, G.; Furthmuller, J., Efficient iterative schemes for ab initio total-energy calculations using a plane-wave basis set. *Phys. Rev. B* **1996,** *54* (16), 11169.

39. Kresse, G.; Hafner, J., Abinitio Molecular-Dynamics for Liquid-Metals. *Phys. Rev. B* **1993,** *47* (1), 558.

40. Blöchl, P. E., Projector augmented-wave method. *Phys. Rev. B* **1994,** *50*, 17953.

41. Kresse, G.; Joubert, D., From ultrasoft pseudopotentials to the projector augmented-wave method. *Phys. Rev. B* **1999,** *59*, 1758.

42. Klimes, J.; Bowler, D. R.; Michaelides, A., Chemical accuracy for the van der Waals density functional. *J. Phys. Cond. Mat.* **2010,** *22* (2), 022201.

43. Carrasco, J.; Santra, B.; Klimes, J.; Michaelides, A., To wet or not to wet? Dispersion forces tip the balance for water ice on metals. *Phys. Rev. Lett.* **2011,** *106*, 026101.

44. Gillan, M. J.; Alfe, D.; Michaelides, A., Perspective: How good is DFT for water? *J. Chem. Phys.* **2016,** *144* (13), 130901.

45. Hanke, F.; Dyer, M. S.; Bjork, J.; Persson, M., Structure and stability of weakly chemisorbed ethene adsorbed on low-index Cu surfaces: performance of density functionals with van der Waals interactions. *J. Phys. Cond. Mat.* **2012,** *24* (42), 424217.

46. Grimme, S.; Antony, J.; Ehrlich, S.; Krieg, H., A consistent and accurate ab initio parametrization of density functional dispersion correction (DFT-D) for the 94 elements H-Pu. *J. Chem. Phys.* **2010,** *132* (15), 154104.

47. Tersoff, J.; Hamann, D. R., Theory And Application For The Scanning Tunneling Microscope. *Phys. Rev. Lett.* **1983,** *50* (25), 1998.

48. Lorente, N.; Persson, M., Theoretical aspects of tunneling-current-induced bond excitation and breaking at surfaces. *Faraday Discuss.* **2000,** *117*, 277.